antibiotics

MDPI

Article

Influence of Growth Media on Bacterial Susceptibility to Antimicrobial Metal Ions

Luke C. Hicks [1,†], Matthew J. Urban [1,†], Hailey Y. Maurer [2], Steven J. DiSpirito [3], Maggie Cortes [1,2], Sarah E. Montanti [2,3], Eleanor P.-B. Race [4], Sophia Cozza [5], Kaveesha N. Kulkarni [2], Benjamin R. Carone [1], Valerie J. Carabetta [6], Jeffrey D. Hettinger [3] and Gregory A. Caputo [1,2,*]

[1] Department of Biological & Biomedical Sciences, Rowan University, Glassboro, NJ 08028, USA; carone@rowan.edu (B.R.C.)
[2] Department of Chemistry & Biochemistry, Rowan University, Glassboro, NJ 08028, USA
[3] Department of Physics & Astronomy, Rowan University, Glassboro, NJ 08028, USA; hettinger@rowan.edu (J.D.H.).
[4] Department of Chemistry, Williams College, Williamstown, MA 01267, USA
[5] Department of Chemistry & Chemical Biology, Stevens Institute of Technology, Hoboken, NJ 07030, USA
[6] Department of Biomedical Sciences, Cooper Medical School of Rowan University, Camden, NJ 08103, USA; carabetta@rowan.edu
* Correspondence: caputo@rowan.edu
† These authors contributed equally to this work.

Abstract

Background: Antimicrobial resistance has developed as a significant world health problem, and numerous approaches have been actively studied to address the challenge. Some metals, including silver, copper, and zinc, have emerged as potential alternatives to traditional antibiotics, especially in the context of medical devices and coatings that can be applied to these devices. However, the effective dose and spectrum of activity of these metals have been areas of question for many material scientists, as well as those looking to translate the coatings into clinical trials. Methods: Here, we have evaluated the efficacy of three antimicrobial metals in solution against a panel of clinically relevant bacteria grown in three different growth media types. We used a combination of microbiological approaches, including determining susceptibility by broth microdilution assays, bacterial growth curves, analysis of biofilm mass using crystal violet binding and metabolism using XTT conversion, and analysis of bacterial morphology by scanning electron microscopy. Results: The results demonstrate that not all antimicrobial metals are equally effective in all media types. Across all conditions tested, Ag^{+} ions were the most effective, followed by Cu^{2+} and Zn^{2+}. Notably, Cu^{2+} and Zn^{2+} showed increased variability in MIC against bacteria grown in nutrient broth media, with both increased susceptibility and decreased growth rates for all bacteria tested. Both *E. coli* and *S. aureus* exhibited significantly smaller cell sizes in NB media when treated with metal ions. Bacterial biofilms grown in nutrient broth media exhibited lower metabolic activity and decreased biomass, although not statistically significant in all cases. Importantly, when compared to mammalian cytotoxicity levels, the dramatic effects of media on the MIC values can have significant impact on calculations of effective dosage. Conclusions: These results demonstrate that studies on the antimicrobial efficacy of metal-based antimicrobials, including metal-based coatings, should be viewed through the lens of differential activity depending on the media conditions used.

Keywords: antimicrobial coatings; antimicrobial materials; bacterial growth media; antimicrobial susceptibility

Academic Editors: Zehra Edis, Maria Fernanda N. N. Carvalho and Kwang-sun Kim

Received: 31 August 2026
Revised: 15 October 2026
Accepted: 26 October 2026
Published: 3 November 2026

Copyright: © 2026 by the authors. Licensee MDPI, Basel, Switzerland. This article is an open access article distributed under the terms and conditions of the Creative Commons Attribution (CC BY) license.

1. Introduction

Medical devices are often prone to bacterial contamination infection, which may result in negative outcomes, including revision surgeries, increased healing and recovery times, significant losses in productivity, and even death [1–4]. The negative impact of infection on and around these devices is exacerbated by the continued development of antimicrobial resistance, which can make these device-associated infections significantly more difficult to treat [5,6]. Similarly, the COVID-19 pandemic elicited significant increases in both antimicrobial resistance development and a shocking 51% increase in central line associated bloodstream infections (CLABSIs) and catheter-associated urinary tract infections (CAUTIs) [7–9].

Many groups have focused on the development of coatings on medical devices to prevent or actively combat infections, promote bone or tissue integration, and safeguard device functionality during the implantation procedure [10,11]. There have been a wide variety of chemistries and functionalities used as coatings for different applications, such as hydrophilic polymeric coatings to reduce friction and increase lubricity [12,13]. Polymer and hydrogel coatings have also been extensively utilized as drug-releasing coatings where a small molecule is embedded within the coating material and releases over time [14]. Indwelling orthopedic devices have been coated with various materials such as hydroxyapatite, extracellular matrix components, magnesium, or chitosan to improve osseointegration [15].

Coating devices with an antimicrobial agent has emerged as an attractive option to limit infection rates and thereby limit the development of resistance in these infections. Coatings have been developed based on a variety of chemistries, as well as for a wide range of applications and substrate materials on which the coating is applied. One approach has used traditional antibiotics, such as rifampin and minocycline, to coat the surfaces of catheters used in delivery of anticancer chemotherapeutics [16]. Numerous applications of drug-releasing polymers have been employed which incorporate antibiotics imbedded in a polymer matrix thaat releases the antimicrobial spontaneously or upon environmental triggers [17]. Antimicrobial metals have been incorporated in various molecular compositions, alloys, and often in combination with titanium for application to orthopedic devices [1,11,18,19]. However, there have been significant challenges in the implementation of these metal-based coatings due to safety concerns around effective dosing [20,21].

While metals are widely known and applied as antimicrobial and specifically antibacterial agents, there is still a great deal of uncertainty on the mechanism of action of these ions. Traditional small molecule antibiotics are often developed with inhibition of a specific protein or cellular target as the mechanism of action; however, metal ions are so small and structurally simple that targeted interactions are effectively impossible. As such, metal ions have been indicated to act as antimicrobials by multiple mechanisms with a variety of cellular targets and interactions. Numerous groups have identified ROS generation, protein damage, DNA damage, disruption of transmembrane ion gradients, cell membrane damage, and inhibition of protein synthesis as mechanisms of antimicrobial activity [22,23]. As a result, the growing consensus is that metals ions act through a multifactorial assault on the bacterial cell, inducing damage in multiple areas simultaneously.

When characterizing the antimicrobial activity of molecules and compounds, most assays in the field are focused on the activity of small molecules on planktonic bacterial targets. The assays for antimicrobial susceptibility are governed by the guidelines of global organizations like the Clinical and Laboratory Standards Institute [24] and ASTM

methods E2149, E2799, and E2180 [25]. However, when evaluating the efficacy of medical device coatings or other surface activity, there is significantly less standardization, especially when antimicrobial testing requires creative approaches to how antimicrobial activity is measured [26–29]. These are not always compatible with the exact requirements of published standards, which often include specific test organisms and also open the door to lab-to-lab variations in experimental procedures, which may influence reported antimicrobial efficacy.

Previous results from our lab and others have shown that release rates of metal ions from surfaces can vary dramatically based on the media in which that release occurs [26]. When evaluating the efficacy of metal ions as antimicrobials, the number of ions in solution is a key driver of activity and can thus be directly influenced by media composition. We first evaluated the antimicrobial efficacy of three commonly utilized metals in antimicrobial coatings, silver, copper, and zinc in three different growth media that have been commonly used in the literature, Luria Bertani (LB), Mueller Hinton (MH), and nutrient broth (NB). Using this efficacy data, we evaluated the effects of the metal species on growth kinetics in different media, cellular metabolism, biofilm formation, and overall cellular morphology.

2. Results

2.1. Antimicrobial Activity of Metal Ions

A series of experiments were carried out to determine the effectiveness of metal ions as antimicrobial agents against a panel of Gram-negative and Gram-positive bacteria. The Minimum Inhibitory Concentrations (MICs) and Minimal Bactericidal Concentrations (MBCs) were determined by the standard broth microdilution assay for each metal in LB, NB, and MH. The MIC and MBC results are generally in agreement with one another, with MBC values being equal to or higher than the corresponding MIC value (Tables 1 and 2). $AgNO_3$ is dramatically more effective than the other metals tested, having MIC values of 100μM or lower against all strains tested, while $CuSO_4$ and $ZnSO_4$ were generally 1–2 orders of magnitude higher. As expected, $MgSO_4$ did not exhibit any antibacterial activity at the highest concentration tested of 100 mM. Importantly, the overall trend of MIC values showed that the MIC in NB was generally lower than either MH or LB, with only three exceptions ($AgNO_3$—*K. pneumoniae*, $ZnSO_4$—*A. baumannii,* and *B. subtilis*).

Table 1. Minimal Inhibitory Concentrations.

	$AgNO_3$ (μM)			**$CuSO_4$ (mM)**			**$ZnSO_4$ (mM)**			**$MgSO_4$ (mM)**		
	LB	**MH**	**NB**	**LB**	**MH**	**NB**	**LB**	**MH**	**NB**	**LB**	**MH**	**NB**
E. coli	12.5	12.5	10	5	10	0.25	2.5	2.5	1	>100	>100	>100
K. pneumoniae	6.25	6.25	50	2.5	10	2.5	0.625	2.5	0.313	>100	>100	>100
A. baumannii	100	12.5	100	>10	10	2.5	5	2.5	5	>100	>100	>100
P. aeruginosa	100	12.5	12.5	>10	>10	2.5	>10	>10	>10	>100	>100	>100
B. subtilis	100	50	12.5	10	2.5	0.5	25	1.25	6.25	>100	>100	>100
S. aureus	50	50	25	5	5	0.625	1.25	2.5	0.156	>100	>100	>100

Table 2. Minimal Bactericidal Concentrations.

	$AgNO_3$ (μM)			$CuSO_4$ (mM)			$ZnSO_4$ (mM)			$MgSO_4$ (mM)		
	LB	**MH**	**NB**	**LB**	**MH**	**NB**	**LB**	**MH**	**NB**	**LB**	**MH**	**NB**
E. coli	12.5	12.5	12.5	5	10	1	5	2.5	6.25	>100	>100	>100
K. pneumoniae	6.25	6.25	100	2.5	10	2.5	2.5	2.5	6.25	>100	>100	>100
A. baumannii	50	12.5	100	10	10	5	5	2.5	6.25	>100	>100	>100
P. aeruginosa	62.5	12.5	100	10	>10	2.5	10	>10	>10	>100	>100	>100
B. subtilis	125	100	25	10	5	0.5	25	1.25	50	>100	>100	>100
S. aureus	50	100	50	5	5	0.625	5	5	0.313	>100	>100	>100

The effect of the metal ions on bacterial growth was further evaluated using traditional Kirby-Bauer assays to determine the zone of inhibition (ZOI). The physical size of the ZOI is primarily driven by the efficacy of the compound being tested but can also be influenced by diffusion and media composition. We compared the ZOIs of the panel of bacteria grown on agar plates containing the different media types (Table 3). In these experiments, $MgSO_4$ was excluded since there was no antimicrobial activity determined in the MIC/MBC experiments above. Representative images of the ZOI plates are shown in Figure S1. The results of these experiments support those of the MIC experiments above, in that the ZOIs on NB plates are generally equal to or larger than the zones of inhibition in LB or MH media, a trend that holds across all three metal species tested.

Table 3. Zones of Inhibition (mm).

	LB			**MH**			**NB**		
	$AgNO_3$	$CuSO_4$	$ZnSO_4$	$AgNO_3$	$CuSO_4$	$ZnSO_4$	$AgNO_3$	$CuSO_4$	$ZnSO_4$
E. coli	10.3	10.9	14	9.1	6.9	10.6	12	19.5	22.8
K. pneumoniae	9	7.7	14	8.3	6.6	10.6	10.9	11	16.8
A. baumannii	11.8	9.5	9.7	10	8.5	10.7	11	14.5	11.3
P. aeruginosa	8.4	9.8	11	6.9	7.6	9.2	8.1	15.8	11.2
B. subtilis	10.5	7.8	8.4	8.9	6.8	16.3	8.5	21.2	23.5
S. aureus	11.1	14.5	17.1	9.3	14.3	17.6	12.6	14.7	18.8

The data immediately demonstrate several salient details regarding growth and efficacy in these systems. As shown by the MIC values in Table 1, silver ions are more effective compared to copper or zinc, by several orders of magnitude. As expected, the $MgSO_4$ controls showed no antimicrobial activity up to 100 mM, the highest concentration tested in these assays. Similarly, the influence of growth media was immediately evident in the MIC and MBC values. In almost all cases, the MIC for bacteria grown in NB was lower than that of the same bacterial species grown in LB or MH. A direct comparison of efficacy in different media was carried out by calculating the ratios of MIC values for a given metal in two different media types, shown in Table 4. These comparisons show an overall trend of increased antimicrobial activity, i.e., lower MIC, in NB media. In some cases, the change in MIC between media was 20-fold or higher (e.g., $CuSO_4$ against *E. coli*). In general, the metals tested yield lower MIC values in NB media compared to LB or MH media (the standard media for MIC assays), although the extent of these changes varies by organism and metal.

Table 4. Minimal Inhibitory Concentration Ratios.

	$AgNO_3$			$CuSO_4$			$ZnSO_4$		
	LB/MH	**LB/NB**	**MH/NB**	**LB/MH**	**LB/NB**	**MH/NB**	**LB/MH**	**LB/NB**	**MH/NB**
E. coli	1	1.25	1.25	0.5	20	40	1	2.5	2.5
S. aureus	1	2	2	1	8	8	0.5	8	16

A. baumannii	8	1	0.125	>1	>4	4	1	1	1
P. aeruginosa	8	8	1	>1	>4	1	n.d.	n.d.	n.d.
B. subtilis	2	8	4	4	20	5	20	4	0.2
K. pneumoniae	1	0.125	0.125	0.25	1	4	0.25	2	8

n.d. = not determined.

2.2. Bacterial Growth Kinetics

Based on the MIC and MBC results, bacterial growth kinetics were evaluated for several bacterial strains at various metal concentrations (Figures 1, 2, and S2–S5). For both *E. coli* (Figure 1) and *S. aureus* (Figure 2), all three metal ions exhibited a dose-dependent interaction with the bacteria, with increasing metal concentration resulting in greater inhibition of bacterial growth. The data support the MIC and MBC findings in that across all strains tested, silver was more effective as a growth inhibitor than copper or zinc, as evidenced by the lower concentrations required for inhibition of growth. Similarly, in all cases the antimicrobial effects of metal ions were most impactful in NB media. It should also be noted that all bacterial strains grown in NB media exhibited slower growth rates when compared to LB or MH and did not reach the same cell density in the control samples over the course of the experiments, as evidenced by the lower OD_{600} values in the control samples. In all samples, an aliquot of the culture was plated on plain media after the end time point in the growth curves to confirm viability of the cultures.

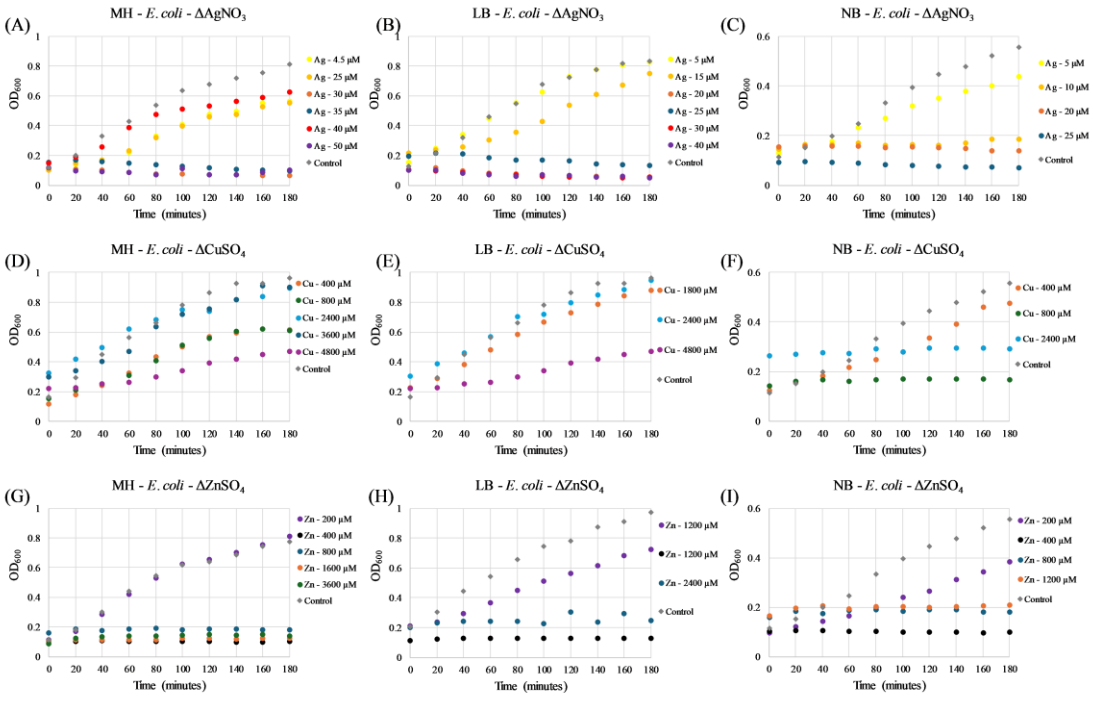


Figure 1. Growth curves of *E. coli* in different media with metals. The bacteria were exposed to differing amounts of $AgNO_3$ (top row), $CuSO_4$ (middle row), or $ZnSO_4$ (bottom row). Bacteria were cultured in either MH (left column; **A**,**D**,**G**), LB (middle column; **B**,**E**,**H**), or NB (right column; **C**,**F**,**I**). Curves are representative of three biological replicates, with the exception of the untreated controls, which are representative of five replicates. Please note the different ranges of metal concentrations in each panel is a result of the differential susceptibility of the bacteria to different metal species under different conditions.

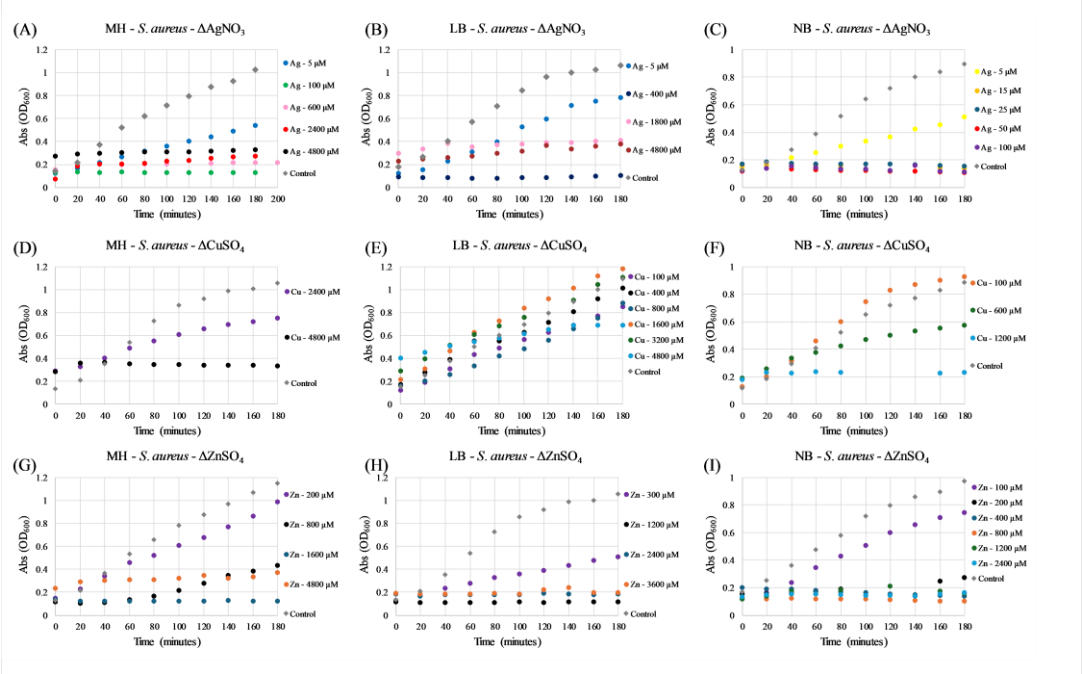


Figure 2. Growth curves of *S. aureus* in different media with metals. The bacteria were exposed to differing amounts of $AgNO_3$ (top row), $CuSO_4$ (middle row), or $ZnSO_4$ (bottom row). Bacteria were cultured in either MH (left column; **A**,**D**,**G**), LB (middle column; **B**,**E**,**H**), or NB (right column; **C**,**F**,**I**). Curves are representative of three biological replicates with the following exceptions: all untreated controls are representative of five replicates, and $AgNO_3$ in LB at 4800 μM is representative of five replicates. Please note the different ranges of metal concentrations in each panel is a result of the differential susceptibility of the bacteria to different metal species under different conditions.

2.3. Bacterial Morphology

Bacterial morphology was investigated using scanning electron microscopy to determine if the media type and metal treatments influenced overall bacterial cell size and shape. If the media composition influenced bacterial growth properties or cellular shape, it could be the underlying cause of the differential sensitivity to the metal ions. Two strains were selected for analysis, *E. coli* and *S. aureus*, as representatives of Gram-negative and Gram-positive species (Figures 3 and 4, respectively). There were very little morphological differences in terms of shape of the cells treated by any of the metals compared to the controls. However, in both *E. coli and S. aureus*, there was significant trend toward smaller average cell size under most treatment conditions when grown in NB media (Figure 5, Table S1). Interestingly, the LB-NB difference is most significant for *E. coli*, while the MH-NB difference is most significant for *S. aureus*. There were no significant differences in cell size for untreated samples in LB, but a significant difference was present in *S. aureus* between MH and NB samples. However, these results arise from a single biological replicate, so additional replicates are needed before conclusive links can be determined. Additionally, the $ZnSO_4$ treated samples exhibited small, irregular aggregates around the cells, which were determined to be Zn-particles by Energy-dispersive Spectroscopy (EDS, Supplementary Figures S8 and S9). Taken together, there is a trend toward smaller cell size in NB media compared to LB and MH when bacteria were exposed to antimicrobial metal ions, and there are likely species-specific preferences that also play into this.

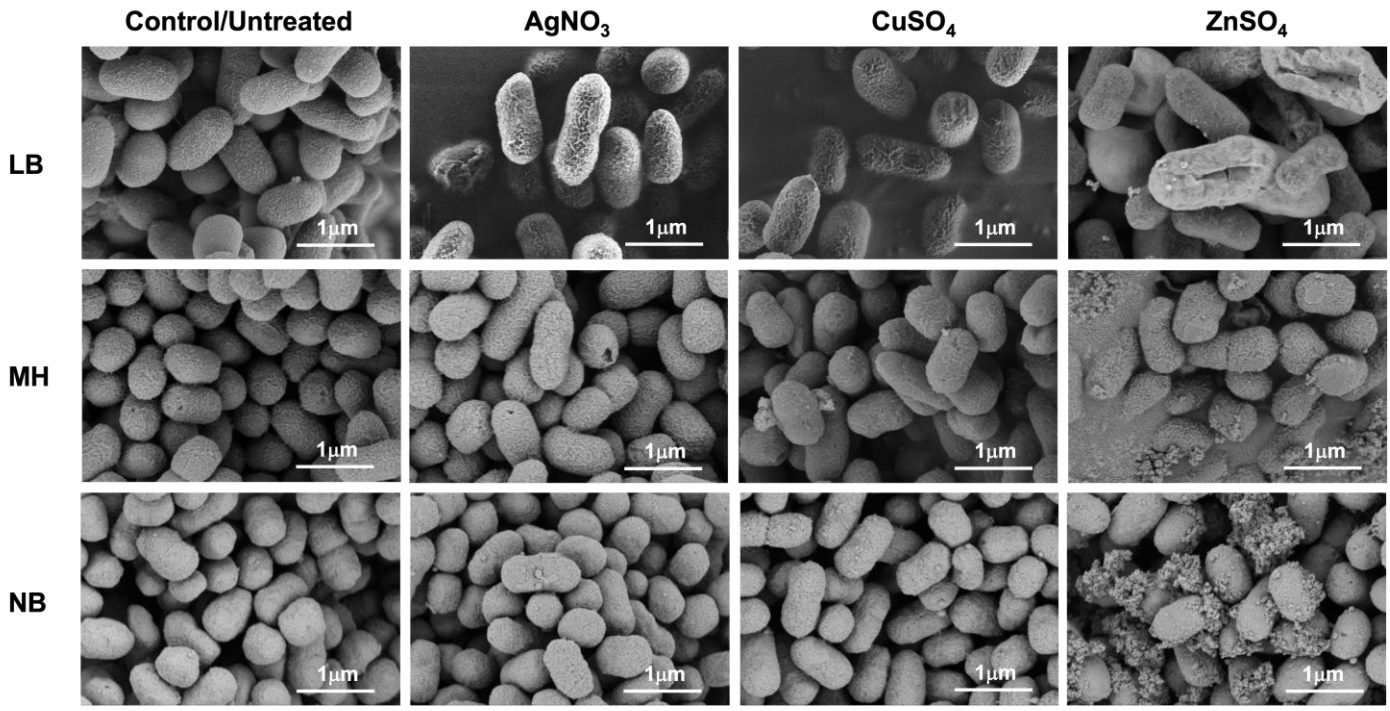


Figure 3. Scanning electron micrographs of *E.coli* grown in LB (top row), MH (middle row), or NB (bottom row) media. Cells were treated with water (left column), $AgNO_3$ (second column), $CuSO_4$ (third column), or $ZnSO_4$ (right column). 1 μm scale bars are at the bottom right of each panel.

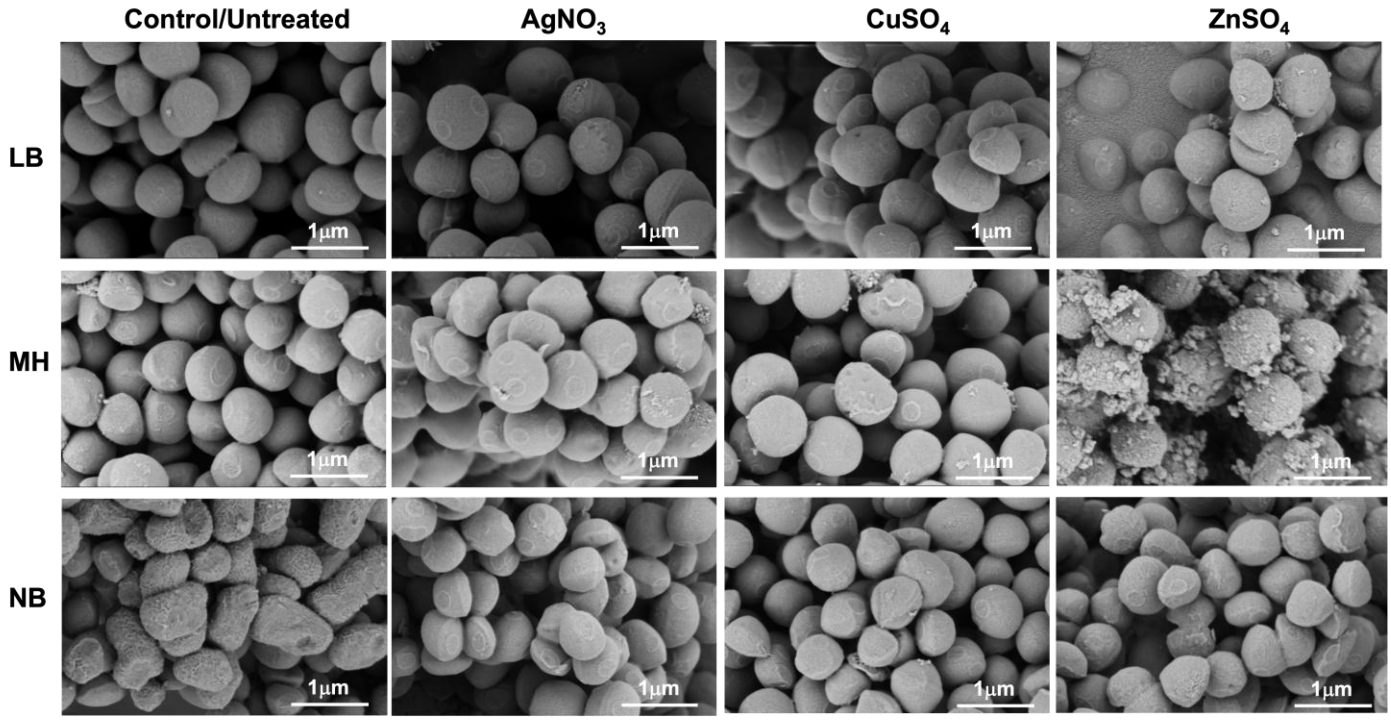


Figure 4. Scanning electron micrographs of *S. aureus* grown in LB (top row), MH (middle row), or NB (bottom row) media. Cells were treated with water (left column), $AgNO_3$ (second column), $CuSO_4$ (third column), or $ZnSO_4$ (right column). 1 μm scale bars are at the bottom right of each panel.

https://doi.org/10.3390/antibiotics15111092

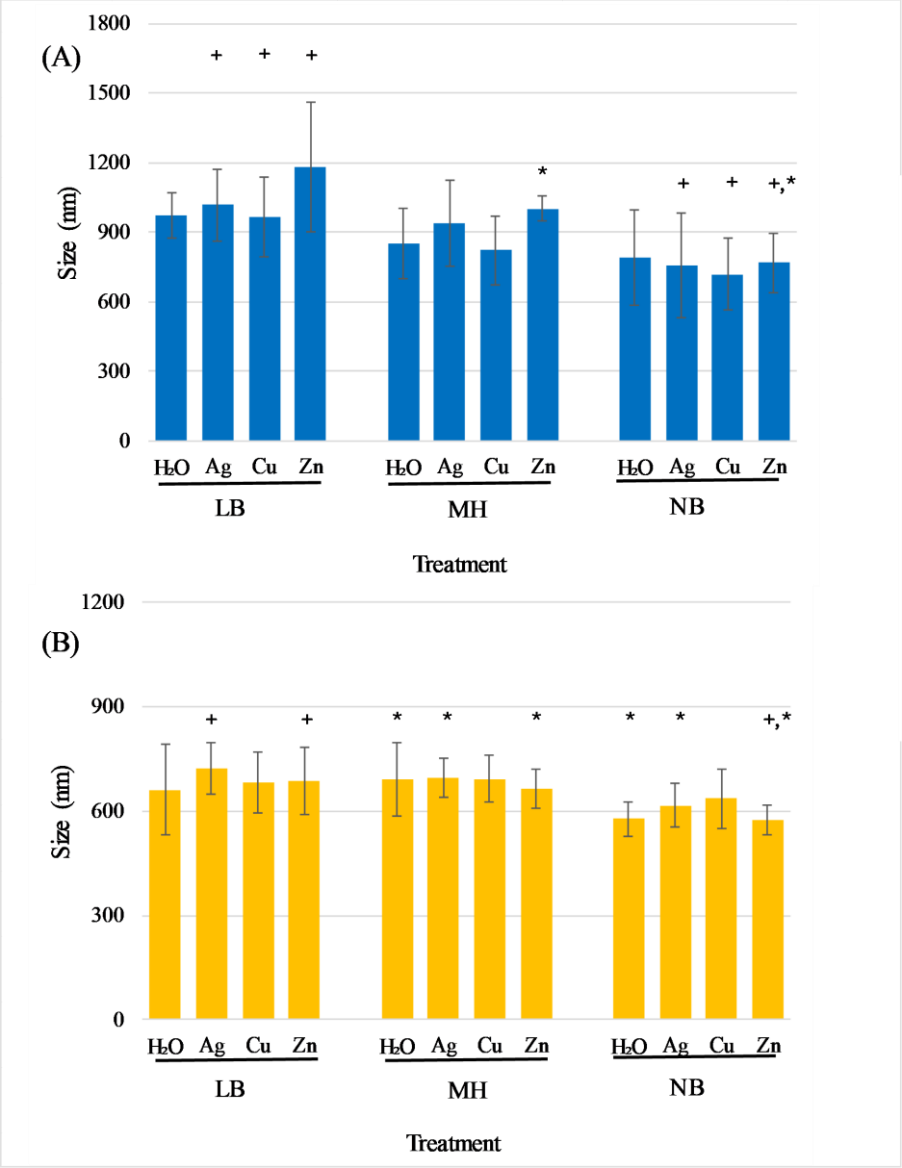


Figure 5. Scanning electron microscopy analysis of cell size. Cell sizes were measured from single biological replicates under each treatment condition in each media type. (**A**) *E. coli* cells measured across the long axis of the cell, (**B**) *S. aureus* cells measured along the equatorial diameter. In all cases, data represent the average of 12 measurements of different bacterial cells from a single biological sample and error bars represent the standard deviation. Statistical significance was determined by a *t*-test, with a *p*-value of <0.05 considered significant. $p < 0.05$ (LB-MH comparison, + = LB-NB comparison, * = MH-NB comparison; note that none of the MH-NB samples were statistically different).

2.4. Biofilm Formation and Inhibition

Based on the results of the growth kinetics experiments above, the effects of the growth media on bacterial biofilm formation were next evaluated. Biofilm metabolic activity is determined using the XTT reduction assay (Figures 6 and S6), while biofilm mass is determined using the crystal violet assay (Figure S7). While these assays exhibit inherent variance, likely due to fluctuations in cell density and replication processes, there are several clear findings from these experiments. Most evident is that biofilms in NB media exhibit lower metabolic activity and that metabolic activity is less responsive to treatment with metal ions. This trend was also evident for biofilm mass in the wells (Figure S7). While most conditions did not show significant differences in biofilm metabolic activity,

for those that were significantly different, the bacteria grown in NB media exhibited the lowest activity (Figures 6 and S6; Tables S2 and S3).

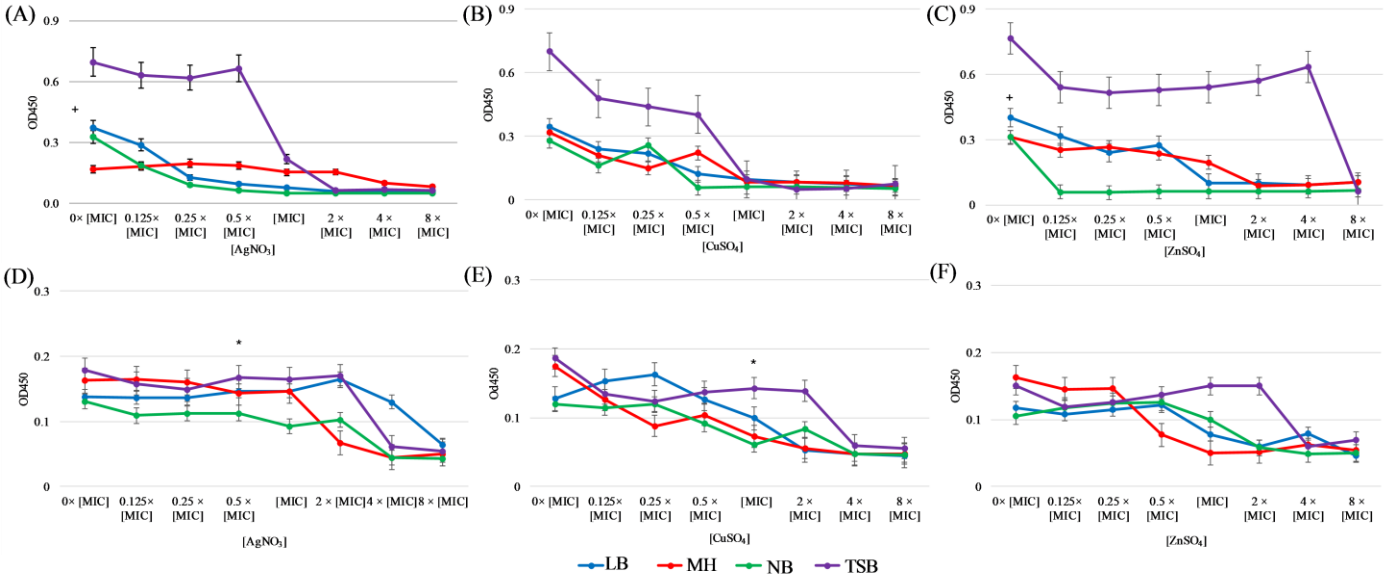


Figure 6. XTT-reduction assay of metabolic activity in biofilm cells (**A–C**) *A. baumannii* average cellular metabolism when in the presence of (**A**) $AgNO_3$, (**B**) $CuSO_4$, (**C**) $ZnSO_4$, and (**D–F**) Methicillin-resistant *S. aureus* (MRSA) average cellular metabolism when in the presence of (**D**) $AgNO_3$, (**E**) $CuSO_4$, (**F**) $ZnSO_4$ in LB (blue), MH (red), NB (green), and TSB (purple) media. Note, the MRSA strain used in these experiments is a clinical isolate and **not** the same *S. aureus* strain used in Figures 2 and 4. Data for each graph consist of averages from 3–5 biological replicates, and error bars represent the standard deviation of these sample sets. Statistical significance was determined by a *t*-test, with *p*-value < 0.05 considered significant. The following designations $p < 0.05$: (LB-MH comparison, + = LB-NB comparison, * = MH-NB comparison; note that none of the MH-NB samples were statistically different).

2.5. Cytotoxicity Analysis

A major underlying factor in the importance of bacterial growth and sensitivity to antibacterial agents is in the application of these agents in clinical settings. In the development of new coatings, devices, and treatments, there is a long and complex series of experiments and evaluations that take place to ensure safety and lack of toxicity to the host. One commonly used metric to screen compounds for biocompatibility at early stages of development is cytotoxicity to cells in culture. Previous results on $AgNO_3$ against red blood cells showed minimal hemolytic activity at concentrations well above the MIC values [26]. This was expanded to screen cytotoxicity against mammalian cells in culture for the metals used in this study. The cytotoxicity data against Tig1 human fibroblasts are shown in Figure 7. As expected, the data show that Mg^{2+} ions had little-to-no effect on cell viability, effectively the same as the negative controls treated with water. The Ag-, Cu-, and Zn-treated samples all induced 50% cell death in the range between 1–10 mM.

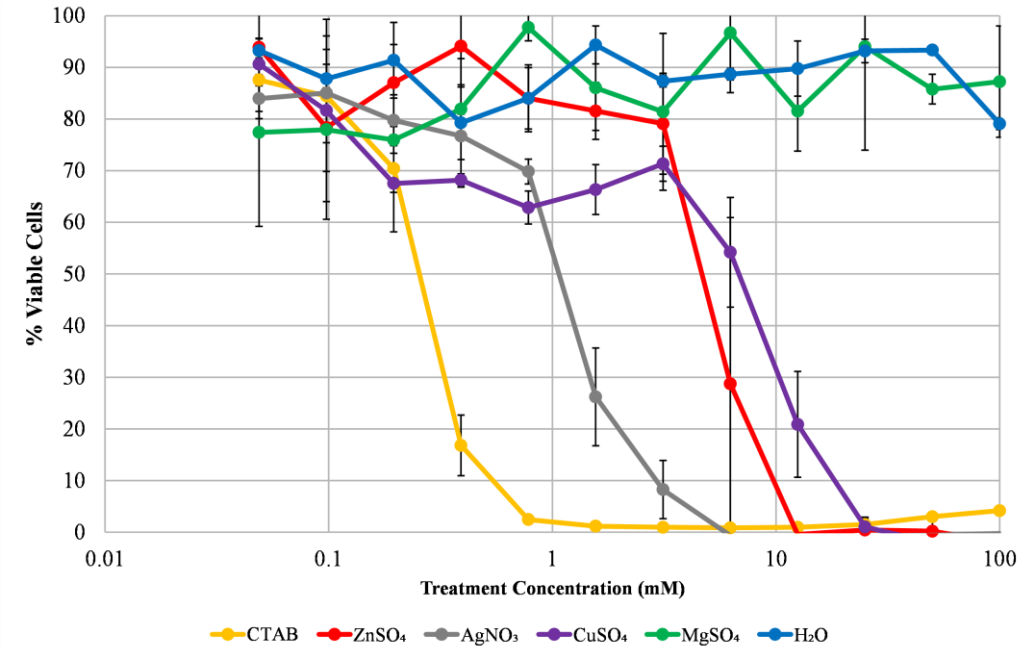


Figure 7. Cytotoxicity against Tig1 human fibroblasts. Average cell viability when screened against $AgNO_3$ (gray), $CuSO_4$ (purple), (C) $MgSO_4$ (green), $ZnSO_4$ (red), CTAB (yellow, positive control), or water (blue, negative control). Experiments were performed in triplicate from independent biological samples, and the values shown are the averages of the triplicates of each respective treatment, with error bars representing the standard deviation.

Using this cytotoxicity data, we calculated an "in vitro selectivity index" for each metal against each bacterial strain tested in Table 5. This was calculated by dividing the approximate concentration, which induced 50% cytotoxicity by the MIC value, similar to the calculation of a therapeutic index. The data are shown in Table 5. The in vitro selectivity index values represent efficacy against bacterial targets as a function of cytotoxic concentration, with higher in vitro selectivity index values meaning a greater difference between antibacterial activity and mammalian cytotoxicity. In vitro selectivity index values below 1.0 indicate that the concentration of metal required for antimicrobial activity is greater than the concentration that caused 50% mammalian cell death. Overall, the highest in vitro selectivity index values were found for silver because of the micromolar efficacy against the bacterial strains tested despite having the lowest calculated IC_{50} against the mammalian cells (Figure 6). This analysis also showed that copper exhibited higher in vitro selectivity index values in NB than LB or MH against all bacteria tested. Zinc exhibited a similar trend to copper comparing NB and LB but showed lower in vitro selectivity index values in NB compared to MH for *A. baumannii* and *B. subtilis*. The variance in calculated in vitro selectivity index values between the media types demonstrates how interpretation of efficacy data can be influenced by bacterial growth media.

Table 5. In vitro selectivity index.

	$AgNO_3$			$CuSO_4$			$ZnSO_4$		
	LB	**MH**	**NB**	**LB**	**MH**	**NB**	**LB**	**MH**	**NB**
E. coli	90.4	90.4	113	1.394	0.697	27.9	1.97	1.97	4.93
K. pneumoniae	180.8	180.8	22.6	2.79	0.697	2.79	7.89	1.97	15.75
A. baumannii	11.3	90.4	11.3	<0.697	0.697	2.79	0.986	1.97	0.986
P. aeruginosa	11.3	90.4	90.4	<0.697	<0.697	2.79	<0.493	<0.493	<0.493
B. subtilis	11.3	22.6	90.4	0.697	2.79	13.94	0.197	3.94	0.789
S. aureus	22.6	22.6	45.2	1.39	1.39	11.15	3.944	1.97	31.6

3. Discussion

Developing novel coating materials for medical devices has been an interest in the medical field for decades. The demands on these coatings vary based on the materials that they are applied to as well as the specific application and usage location of the device. However, despite the significant interest in this area, there is little standardization of testing protocols for these novel materials and coatings because of the varying demands and application goals. This is especially challenging for antimicrobial coatings, as common infectious agents associated with devices can vary based on the location and application of the device [2,30]. Metals have long been investigated as a potential component of antimicrobial coatings and surfaces because they exhibit antimicrobial activity [31]. For many applications, metal nanoparticles are the major active component of the antimicrobial composition, including several compositions of silver or ceramic nanoparticles [32]. Nanoparticles can function through a variety of mechanisms, but antimicrobial activity is associated with released metal ions. Thus, most of the active species remain trapped within the nanoparticle and are subject to bulk forces that drive dissolution [33,34].

There has been significant research on the effect of environmental stimuli, nutrients, and environmental conditions on bacterial growth [35–39]. It is well established that different bacteria grow optimally based on macronutrient and micronutrient availability and specific temperature ranges for a given species. These foundational microbiological studies have expanded into evaluating the effectiveness of antimicrobials as a function of growth conditions. There are numerous instances where bacteria exhibit increased tolerance to conventional antimicrobials, often due to the specific antibiotic target being less active when the bacteria are not actively dividing or are present in a biofilm [40]. However, the susceptibility to some antibiotics inversely correlates with bacterial growth, presumably because the bacteria can respond to antimicrobial insults through a variety of mechanisms, which are all options because the cells have abundant resources available for protein synthesis and gene expression. Notably, *P. aeruginosa* requires high nutrient conditions to produce efflux pumps in response to tetracycline treatment [41]. Importantly, expression of efflux pumps is the primary mechanism for bacteria to respond and combat exposure to the metal ions used in this study. Beyond efflux pumps, redox stress-response pathways have also been shown to be a mechanism for active response to metal exposure and are also negatively impacted by nutrient limitation [42,43]. Similarly, Wu and coworkers demonstrated that tea-derived polyphenols exhibited 4- to 64-fold increases in MIC against bacteria grown in robust, complex media as opposed to chemically defined medium [44]. In another study, Wand and colleagues demonstrated that the antimicrobials colistin and polymyxin B exhibited significantly higher MIC values in MHII media when compared to TSB [45]. Most recently, the phenomenon was demonstrated to extend to multiple Mycoplasma species, where *Mycoplasma gallisepticum* and *Mycoplasma synoviae* showed differential growth rates in different media compositions and variable MIC values against multiple traditional antimicrobials such as doxycycline, erythromycin, and tilmicosin [46].

The role of media composition on metals in the solution has been studied for decades. One of the earliest studies evaluated metal ion availability in different media using electrochemical measurements [47]. Those results showed that metals were complexed to different extents when added to complex growth media. Notably, copper was extensively complexed by NB media, yielding very low amounts of Cu^{2+} ions, the antimicrobially active form, available in solution. Our results parallel these findings with bacteria exhibiting decreased MIC values in NB broth, which could result from less Cu^{2+} ions being available to interact with the bacteria. However, full metal speciation and analysis of the chelators and counterions present in NB would be required for identifying a causal link. More recently, the same metal ions tested in the work presented here were evaluated with

different media compositions [48]. Their results for MH and LB broth parallel the results shown in Tables 1 and 4, with similar MIC values between the two media types. The overall trend holds that in rich media like LB, the MIC values are generally higher than in poorer media such as NB is consistent. Similar results for silver ions against *B. subtilis* were reported where increasing concentrations of yeast extract, Cl^- ions, and S^{2-} ions mitigated the efficacy of silver ions [49]. Our results are consistent with these findings as well, with the MIC values against all bacteria in LB, which contains added NaCl as a media component, being equal or higher than those in MH and NB, which do not contain added NaCl. These results indicate that the Ag susceptibility changes observed in our studies may be partially driven by Ag^+ ion availability and solubility, which is influenced by the presence of Cl- ions.

These results lead to the question of what is causing the changes in the efficacy of the metal ions. Based on the results of the XTT metabolic assay performed here, the overall metabolic state of the bacteria under biofilm conditions may be playing a role leading to this difference in sensitivity. Clearly, under all conditions tested, the bacteria grown in NB media exhibited less metabolic activity under biofilm conditions (Figures 6 and S6), which correlates with and supports the results of the growth kinetics experiments. It should be noted that while these results parallel one another, there are a wide range of metabolic differences for bacteria when in a biofilm compared to growing planktonically as in the growth curve experiments. As such, these results should not be strictly directly compared. Importantly, the NB-cultured strains also exhibited a trend toward lower biofilm mass (Figure S7), although not statistically significant in most cases. The biofilm results are consistent with the findings of numerous groups that media composition can have effects on biofilm formation by *S. aureus*, *E. coli*, *Enterococcus faecalis*, *Salmonella enterica*, and *P. aeruginosa* [50–53]. Taken together, these results imply that the bacteria are nutritionally deficient in NB compared to other media types, perhaps impairing the ability to respond and counteract the action of the metal ions. However, more in-depth experimentation on cellular metabolism under biofilm conditions and metabolic intermediates under metal-treated conditions would be necessary to determine a causal link between basal metabolism and susceptibility.

Metal ion speciation in the media likely plays a contributing role to antimicrobial susceptibility. Earlier work demonstrated that media composition can have effects on release rate of silver ions from solid surfaces, with chemical complexity of the medium inversely correlating with release rates. The change in release rate is most likely caused by the formation of a passivation layer at the metal surface through ion interactions resulting in insoluble or sparingly soluble salts. Those studies used sample preparation methods that were able to assess all Ag atoms in solution, regardless of their speciation or complexation with other molecules or chelators. The antibacterial efficacy studies presented in this work and others are preferential for the active form of the metal, i.e., the metal ion [48,49]. The media compositions used in this study all contain significant amounts of similar undefined media building blocks, including tryptone (LB), yeast extract (LB and NB), peptone (NB), and casein hydrolysate (MH). Media components such as tryptone, yeast extract, S^{2-}, and PO_4^{3-} had the most significant effects on bacterial growth and metal ion susceptibility [48,49]. The study presented here is unable to evaluate the effects of this variable since only LB and NB have one common component. The variable nature of the undefined components can potentially influence availability and efficacy of metal ions. The work presented here expands upon previous studies, demonstrating that growth-rate reductions and metal ion sensitivity are common among multiple strains of bacteria, and the effect is present, although to differing degrees, for different metal ions. These changes in susceptibility may be related to the differing ionic conditions in the growth media, specifically the presence of differing amounts of counterions and chelators that could alter

the solubility and availability of the metal ions tested. For example, increased Cl- concentrations mentioned above likely result in the formation of some insoluble AgCl, while the insoluble Zn-containing clusters were observed by SEM (and EDS measurements) in differing extents in different media types, although the presence of these structures did not correlate to MIC values (Figure S8). Direct measurement of metal ion speciation, known chelator concentrations, soluble metal concentrations, and metal uptake into bacteria are necessary to clearly determine the role of metal ion availability to antimicrobial activity.

All bacteria investigated were able to reach saturation density and exist as viable cultures in all media tested. The results presented here demonstrate that among the three media types tested, copper antimicrobial activity is the most susceptible to differences in media composition, in some cases 20- to 40-fold lower in NB compared to MH or LB. Additionally, our results show that MIC values determined in LB are generally increased for Ag, likely due to the complexation of Ag^{+} with Cl^{-} ions in the medium. The complex mixtures of media can clearly affect both the growth rate and susceptibility to metal ions as antimicrobials. Based on the XTT and CV assays, there were very few cases where there were significant differences in biofilm formation between LB and MH media. The most common cases where statistically significant differences in CV or XTT results involved a difference between NB media and either LB or MH. Importantly, the differences in cell morphology were more significant, in that the bacterial cell sizes observed in treated samples were significantly different in NB compared to MH and LB. Interestingly, the largest differences were between LB and NB for *E. coli* and MH and NB for *S. aureus* with both cases exhibiting smaller cell sizes in NB broth. However, there were no significant differences in cell size in the untreated samples, indicating that the media effects only exist or are amplified when the bacteria are under stress from the metal antimicrobials. However, this is only a preliminary analysis stemming from a single biological replicate for each set of conditions, so further study is necessary before forming conclusive relationships. While all three media are clearly viable options for antibacterial studies, the results demonstrate that judicious selection of media for these studies is critical for proper interpretation of results, as well as comparison between studies from different research groups.

Study Limitations: There are several limitations to the study as presented that should be considered and can guide the development of future experiments. The direct measurement of metal speciation was not performed. As discussed above, metal speciation can affect metal ion solubility in the aqueous media used in this study as well as altering bioavailability. As such, it is impossible to determine what concentration of the metals were available to the bacteria, as well as how much the bacteria absorbed. Similarly, bacterial responses such as ROS responses and expression of genes linked to resistance mechanisms were not directly investigated. The in vitro selectivity index was determined using only 1 mammalian cell line, which would need further testing against a panel of cell types before using this as an indicator for additional studies involving animal models. Additionally, this study was designed to have a broad scope across multiple bacterial species, foregoing the analysis of multiple strains of the same species. This excludes the possibility of identifying strain-specific differences that may respond to media conditions and/or metal exposure. Finally, as with all in vitro-based experimentation, the data are not directly indicative of suitability and translation for medical device coatings. Another limitation is the lack of availability of full elemental analyses of the commercial media used for bacterial growth. While there are bound to be lot-to-lot differences due to the biological sources of the nutrient materials, an in-depth evaluation of composition requires in-house determination. The studies presented here were designed to continue to inform researchers on some of the subtleties of using metal ions as antimicrobials and the influence of the media on the analysis.

4. Materials and Methods

4.1. Materials

Liquid and solid bacterial culture media were from EMD (LB, currently Sigma catalog number L3522; St. Louis MO, USA), Criterion (MH, catalog number C7521; Hardy Diagnostics, Santa Maria CA, USA), and BD Biosciences Difco (NB, catalog number 233000; Franklin Lakes, NJ, USA). Metal salts and buffers were from VWR (Radnor PA, USA) and dissolved in distilled water before use. In addition, 2,3-Bis-(2-Methoxy-4-Nitro-5-Sulfophenyl)-2*H*-Tetrazolium-5-Carboxanilide (XTT) and crystal violet (CV) were from VWR and dissolved in dimethylformamide (XTT) or deionized water (CV). Hexamethyldisilane (HDMS) and paraformaldehyde for electron microscopy were from Sigma-Aldrich.

4.2. Bacterial Strains and Culturing

Bacterial strains *Escherichia coli* D31 (CGSC 5165), *Staphylococcus aureus* (ATCC 35556), *Pseudomonas aeruginosa* PA-01 (ATCC 47085), *Acinetobacter baumannii* (ATCC 19606), *Bacillus subtilis* (ATCC 6051), and *Klebsiella pneumoniae* (ATCC 700603) [54] were stored as glycerol stocks at −80 °C until use. Deidentified methicillin-resistant *S. aureus* (MRSA) strains were acquired from the clinical microbiology laboratory at Cooper University Hospital, Camden, NJ, USA. This strain was identified and characterized by drug susceptibility tests, VITEK 2, and mass spectrometry. Each bacterial species was first streaked across LB-Miller agar plates. Single colonies were inoculated into fresh growth media and incubated within a shaking incubator at 220 RPM at 37 °C for 18 h. Following inoculation, bacteria were diluted 1:200 and grown to an optical density at 600 nm (OD_{600}) of 0.220130.6, which is within the logarithmic growth phase. Next, the culture was diluted across several sets of sterile glass test tubes—1 mL of culture diluted into 2 mL of fresh media, producing a 3 mL sample. Test tubes were established in triplicate with multiple metal ion concentrations surveyed throughout each experiment. Bacterial cultures had absorbance measured every 20 min over a 3 h period. After 3 h, 10 µL of each tube were transferred onto their own agar petri dish of the same growth medium as used during the experiment, spread, incubated overnight at 37 °C, and visually inspected/imaged the following day for bacterial growth.

4.3. Minimal Inhibitory Concentration and Minimal Bactericidal Concentration Determination by Broth Microdilution

Bacterial growth inhibition and cell death were assessed with the traditional broth microdilution assay, derived from the CLSI method [55,56]. Cultures were incubated overnight and subsequently diluted into fresh media. Cultures were grown to an OD_{600} 0.2–0.6 and were diluted to a final cell density of ~5×10^5 CFU/mL for the experiment. Cultures were diluted based on previously published OD_{600} to colony-forming units per mL (CFU/mL) conversion factors that $OD_{600} = 1.0$ is equivalent to ~1×10^9 CFU/mL for *A. baumannii*, ~2×10^8 CFU/mL for *P. aeruginosa*, ~2×10^8 CFU/mL for *B. subtilis*, and ~2×10^9 CFU/mL for *K. pneumoniae*, ~1×10^9 CFU/mL for *E. coli*, and ~5×10^8 CFU/mL for *S. aureus* [57–62]. These values were determined in LB and MH media and were extended to the bacterial cultures grown in NB. Exact CFU/mL to OD_{600} relationships in NB were not performed. Treatments were aliquoted from a template 96-well plate with serial dilutions from a top row concentration down to a control containing only deionized water with no treatment. Starting concentrations varied depending on the metal being tested, with a highest concentration of 100 µM for $AgNO_3$ and 100 mM for $CuSO_4$, $ZnSO_4$, and $MgSO_4$. Each dilution was 2-fold lower than the row above. In cases where no MIC could be determined because all tested concentrations inhibited growth, experiments were repeated

with 4× dilution to the starting (highest) concentration, e.g., the next experiment would start with 25 μM of $AgNO_3$. Bacterial cultures were added to a final concentration of ~5 × 10^5 CFU/mL in a final volume of 200 μL on the experiment plate. Experiments were performed in at least triplicate from biological replicates. The plate was incubated at 37 °C for 18 h. After incubation, the OD_{600} of each well was measured using a Spectramax M5 multimode plate reader (Molecular Devices, San Jose CA, USA). MIC was defined as the consensus of the lowest concentration of treatment that prevented bacterial growth as judged by turbidity, with $OD_{600} < 0.1$ being the cutoff value used for no bacterial growth [63]. Subsequently, 1 μL of each well was aliquoted onto a petri dish containing the same agar type that corresponds to the growth medium tested, i.e., MICs performed with MH-cultured bacteria had bacteria transferred onto an MH agar plate. Agar plates were incubated overnight at 37 °C, and images were collected the following morning. MBC was defined as the consensus concentration of treatment that prevented bacterial growth on the agar plate from of three biological replicates. In all cases, the MBC values were within 1 dilution of each other between biological replicates.

4.4. Kirby-Bauer Test

The Kirby-Bauer test was used as previously described with minor changes [64]. Overnight cultures were prepared as above, diluted the following day, and incubated at 37 °C until $OD_{600} = 0.2$. Next, 50 μL of culture were used to inoculate agar plates containing either LB, NB, or MH media as nutrient source, and spread using glass beads. After 10 min of incubation to ensure bacterial adhesion, filter paper discs containing 20 μL of metals from a 1 mM stock solution or water as a control were placed onto the agar plate and allowed to incubate overnight for a total of ~18 h at 37 °C. After incubation, the zone of inhibition was measured in mm, using digital calipers, and the plate was imaged using digital photographs.

4.5. Biofilm Formation Protocol

Overnight cultures were prepared as above. The next day, overnight cultures were diluted to an OD_{600} of 0.1 and added to the plate, which contained a 2-fold dilution series of the metals at concentrations corresponding to 8× MIC down to 0.125× MIC, and an untreated well. Plates were then incubated at 37 °C for 48 h.

4.6. Biofilm Mass Analysis by Crystal Violet

Planktonic cells were removed from the biofilm plates by aspiration. Wells were washed 3x with 200 μL of phosphate buffered saline (PBS, 10 mM sodium phosphate, 150 mM NaCl, pH 7.2), which was removed by aspiration after each wash step. Next, 200 μL of 0.1% (*w*/*v*) crystal violet solution was added to each well and incubated at room temperature for 20 min, followed by four additional rounds of washing with PBS. After removing the final wash, plates were allowed to incubate overnight to allow evaporation of any remaining PBS. The next morning, 250 μL of destaining solution (80% ethanol, 20% acetic acid) were added to each well and incubated at room temperature for 15 min. After incubation, contents of the wells were mixed by pipetting, and 100 μL were transferred to a new 96-well plate. Absorbance of CV was measured at 550 nm. All assays were performed with six technical replicates in at least in triplicate biological replicates.

4.7. Biofilm Metabolism Assay by XTT

Planktonic cells were removed from the biofilm plates by aspiration. Wells were washed 3× with 200 μL of PBS, which was removed by aspiration after each wash step. Next, 200 μL of PBS and 12 μL of XTT-menadione solution (0.833 mg/mL XTT, 660 μM menadione, final concentrations) were added to each well and incubated at room

temperature for 20 min. The XTT stock was prepared in PBS, and the menadione stock was prepared in dimethyl formamide. The stock concentration of XTT should be 1 mg/mL, and the stock concentration of menadione should be 0.174 M. Plates were covered and wrapped in aluminum foil (including lid) and allowed to incubate overnight at 37 °C. The next day, the absorbance of each well was measured at 450 nm. All determinations were made in at least biological triplicates, with six technical replicates and error bars reported represent standard deviations.

4.8. Scanning Electron Microscopy (SEM)

The bacteria were cultured in three broth types: LB, NB, and MH. Each culture was then grown to an OD_{600} of 0.15–0.45 and divided into four sample groups. The cultures were exposed to either water (negative control), $AgNO_3$, $ZnSO_4$, or $CuSO_4$. The samples were then incubated at room temperature for 1 h and the bacteria isolated from the medium by centrifugation. The supernatant was removed, the pellet was then resuspended in 1 mL of 4% paraformaldehyde, and then the samples were centrifuged again, with the supernatant being removed. The samples were then dehydrated by adding 1 mL of ethanol at 50%, 60%, 70%, 80%, 90%, and 100% concentrations with the concentration increasing by 10% after each repeated centrifugation step. Once 100% ethanol was used to resuspend the pellet, 9 mL of 100% ethanol were added to make a 1:10 dilution of the sample. Each sample was centrifuged for 60 min at 14000 rpm using an ALLEGRA X-14R (Beckman-Coulter Life Sciences, Indianapolis, IN, USA) at 20 °C to form a pellet. Solvents were removed using a micropipette, leaving only the pellet. The pellets were then stained by applying 1 mL of hexamethyldisilane (HDMS) for 20 min. The HDMS was removed, and the pellets were placed in a hood for 12 h to allow the residual HDMS to evaporate. The samples were then mounted on stubs, made more conducting using 10 nm of sputtered with 10 nm of Au, and imaged in an Apreo S scanning electron microscope (Thermo Fisher, Waltham, MA, USA) using approximately a 3 mm working distance, and an acceleration potential of between 2 and 3 kV. Images were collected using the T1 in-lens backscattered electron detector. Measurements were taken from individual frames of biological replicates, depending on the sample. Measurements of cell size were performed using the xT Microscope Control) software (v13.9.1).

4.9. Mammalian Cell Cytotoxicity

Tig1 human fibroblast cells (Coriell:AG06173) were incubated in DMEM media with 10% FBS at 37 °C until 80–95% confluency was attained. Once the proper confluency level had been reached, the fibroblasts were trypsinized and aspirated to create a homogeneous mixture. Then, 1 mL of cells was added to 20 mL of DMEM media. Next, 180 µL of the cell suspension were added to each well of a 96-well plate containing serially diluted compounds. The plate was incubated for 24 h at 37 °C, followed by the addition of 20 µL of CellTiter-Blue to each well, and incubated for an additional 18–24 h. The absorbance was measured at 590 nm.

4.10. Statistical Analysis

Biofilm Assay Statistical Analysis—Absorbance data were analyzed using a linear mixed-effects model in JMP (JMP Statistical Discovery LLC; Cary, NC, USA). Technical replicates were averaged for each biological replicate and experimental condition prior to analysis. Media, treatment concentration, and their interaction were included as fixed effects, while biological replicate was included as a random effect to account for variation among independent biological replicates. Models were fitted using the Fit Model platform, and the significance of fixed effects was assessed using the corresponding *t*-tests. Where appropriate, pairwise comparisons were performed to evaluate differences in

absorbance between media across treatment concentrations. *p*-values were tabulated, and statistically significant results were highlighted to facilitate interpretation. Statistical significance was defined as $\alpha = 0.05$.

Scanning Electron Microscopy Statistical Analysis—Pairwise comparisons of bacterial size between growth media were performed separately for each metal treatment ($AgNO_3$, $CuSO_4$, $ZnSO_4$, and H_2O) and bacterial type (*E. coli* and *S. aureus*) using two-sided Welch's *t*-tests based on summary statistics (mean, standard deviation, and sample size, $n = 12$). Welch's *t*-test was used to account for potential differences in variance between groups. *p*-values were adjusted using the Holm–Bonferroni method to correct for multiple comparisons, with adjustments applied separately to the three pairwise media comparisons within each metal treatment and bacterial type. *p*-values were tabulated, and statistically significant results were highlighted to facilitate interpretation. Statistical significance was defined as $\alpha = 0.05$.

5. Conclusions

The results presented here demonstrate that among the three media types tested (LB, MH, NB), the antimicrobial activity of copper is the most susceptible to differences in media composition. These effects are likely a combination of differences in bacterial metabolism in the different media types, as well as contributions from metal—ion interactions with media components.

Supplementary Materials: The following supporting information can be downloaded at: https://www.mdpi.com/article/10.3390/antibiotics15111092/s1, Figure S1: ZOI images, Figures S2–S5—Growth curves, Figure S6—additional XTT assays, Figure S7—biofilm mass analysis by crystal violet assay, Figures S8 and S9–EDS analysis of SEM images, Tables S1–S3–*p*-values from statistical analysis.

Author Contributions: Conceptualization, G.A.C. and J.D.H.; investigation, L.C.H., M.J.U., H.Y.M., M.C., K.N.K., E.P.-B.R., S.J.D., S.C. and S.E.M.; writing—original draft preparation, L.C.H. and G.A.C.; writing—review and editing, L.C.H., M.J.U., B.R.C., V.J.C., J.D.H. and G.A.C.; visualization, L.C.H., M.J.U. K.N.K. and S.J.D.; supervision, B.R.C., V.J.C., J.D.H. and G.A.C.; project administration, B.R.C., V.J.C., J.D.H. and G.A.C. All authors have read and agreed to the published version of the manuscript.

Funding: This research received no external funding.

Institutional Review Board Statement: Not applicable.

Informed Consent Statement: Not applicable.

Data Availability Statement: The raw data supporting the conclusions of this article will be made available by the authors on request as a repository is not currently available for this information.

Conflicts of Interest: The authors declare no conflicts of interest.

Abbreviations

The following abbreviations are used in this manuscript:

CFU	Colony Forming Units
CV	Crystal Violet
DMEM	Dulbecco's Modified Eagle Medium
FBS	Fetal Bovine Serum
LB	Luria-Bertani
MBC	Minimal Bactericidal Concentration
MIC	Minimal Inhibitory Concentration
MH	Mueller-Hinton

NB	Nutrient Broth
OD_{600}	Optical Density @ 600 nm
PBS	phosphate buffered saline
ROS	Reactive oxygen species
SEM	Scanning Electron Microscopy
XTT	2,3-Bis-(2-Methoxy-4-Nitro-5-Sulfophenyl)-2*H*-Tetrazolium-5-Carboxanilide
ZOI	Zone of Inhibition

References

1. Cao, H.; Qiao, S.; Qin, H.; Jandt, K.D. Antibacterial Designs for Implantable Medical Devices: Evolutions and Challenges. *J. Funct. Biomater.* **2022**, *13*, 86. https://doi.org/10.3390/jfb13030086.
2. Garvey, M. Medical Device-Associated Healthcare Infections: Sterilization and the Potential of Novel Biological Approaches to Ensure Patient Safety. *Int. J. Mol. Sci.* **2024**, *25*, 201. https://doi.org/10.3390/ijms25010201.
3. Mishra, A.; Aggarwal, A.; Khan, F. Medical Device-Associated Infections Caused by Biofilm-Forming Microbial Pathogens and Controlling Strategies. *Antibiotics* **2024**, *13*, 623. https://doi.org/10.3390/antibiotics13070623.
4. Mourad, S.; Salah, A.N.; Mansour, R.M.; Elesawy, A.E.; El-Sayyad, G.S.; Mohammed, O.A.; Sayed, G.A.; Elshami, N.H.; Abdel Mageed, S.S.; Farahat, N.M.; et al. Collateral Damage: The Hidden Cardiovascular Consequences of Antibiotic Resistance. *Compr. Physiol.* **2026**, *16*, e70214. https://doi.org/10.1002/cph4.70214.
5. CDC. *Antibiotic Resistance Threats in the United States, 2019*; U.S. Department of Health and Human Services, CDC: Atlanta, GA, USA, 2019.
6. World Health Organization. *Global Antibiotic Resistance Surveillance Report 2025: WHO Global Antimicrobial Resistance and Use Surveillance System (GLASS)*, 1st ed.; World Health Organization: Geneva, Switzerland, 2025.
7. Fakih, M.G.; Bufalino, A.; Sturm, L.; Huang, R.H.; Ottenbacher, A.; Saake, K.; Winegar, A.; Fogel, R.; Cacchione, J. Coronavirus disease 2019 (COVID-19) pandemic, central-line-associated bloodstream infection (CLABSI), and catheter-associated urinary tract infection (CAUTI): The urgent need to refocus on hardwiring prevention efforts. *Infect. Control Hosp. Epidemiol.* **2022**, *43*, 26–31. https://doi.org/10.1017/ice.2021.70.
8. Petrakis, V.; Panopoulou, M.; Rafailidis, P.; Lemonakis, N.; Lazaridis, G.; Terzi, I.; Papazoglou, D.; Panagopoulos, P. The Impact of the COVID-19 Pandemic on Antimicrobial Resistance and Management of Bloodstream Infections. *Pathogens* **2023**, *12*, 780. https://doi.org/10.3390/pathogens12060780.
9. Yek, C.; Mancera, A.G.; Diao, G.; Walker, M.; Neupane, M.; Chishti, E.A.; Amirahmadi, R.; Richert, M.E.; Rhee, C.; Klompas, M.; et al. Impact of the COVID-19 Pandemic on Antibiotic Resistant Infection Burden in U.S. Hospitals. *Ann. Intern. Med.* **2025**, *178*, 796–807. https://doi.org/10.7326/ANNALS-24-03078.
10. Botterill, J.; Khatkar, H. The role of hydroxyapatite coating in joint replacement surgery—Key considerations. *J. Clin. Orthop. Trauma* **2022**, *29*, 101874. https://doi.org/10.1016/j.jcot.2022.101874.
11. Cyphert, E.L.; von Recum, H.A. Emerging technologies for long-term antimicrobial device coatings: Advantages and limitations. *Exp. Biol. Med.* **2017**, *242*, 788–798. https://doi.org/10.1177/1535370216688572.
12. Do Nascimento, R.M.; Figueiredo Soares Rodrigues, J.E.; de Vasconcellos, A.; da Silva, D.A.; Bedin, R.G.; Martins Machado, J.P.; Ramos, A.P.; Rangel, E.C.; Furini, L.N.; Rosso Dotto, M.E.; et al. Surface Energy and Pinning Forces of Fluorine-Free, Water-Friendly Coatings for Medical Devices. *Langmuir* **2026**, *42*, 2688–2700. https://doi.org/10.1021/acs.langmuir.5c05278.
13. Wang, S.; Li, J.; Ren, F.; Zhang, J.; Song, W.; Ren, L. New Dawn in the Treatment of Rheumatoid Arthritis: Advanced Insight into Polymer Hydrogel Research. *Gels* **2025**, *11*, 136. https://doi.org/10.3390/gels11020136.
14. Borandeh, S.; van Bochove, B.; Teotia, A.; Seppala, J. Polymeric drug delivery systems by additive manufacturing. *Adv. Drug Deliv. Rev.* **2021**, *173*, 349–373. https://doi.org/10.1016/j.addr.2021.03.022.
15. Bohara, S.; Suthakorn, J. Surface coating of orthopedic implant to enhance the osseointegration and reduction of bacterial colonization: A review. *Biomater. Res.* **2022**, *26*, 26. https://doi.org/10.1186/s40824-022-00269-3.
16. Chemaly, R.F.; Sharma, P.S.; Youssef, S.; Gerber, D.; Hwu, P.; Hanmod, S.S.; Jiang, Y.; Hachem, R.Y.; Raad, II. The efficacy of catheters coated with minocycline and rifampin in the prevention of catheter-related bacteremia in cancer patients receiving high-dose interleukin-2. *Int. J. Infect. Dis.* **2010**, *14*, e548–552. https://doi.org/10.1016/j.ijid.2009.08.007.
17. Negut, I.; Bita, B.; Groza, A. Polymeric Coatings and Antimicrobial Peptides as Efficient Systems for Treating Implantable Medical Devices Associated-Infections. *Polymers* **2022**, *14*, 1611. https://doi.org/10.3390/polym14081611.
18. Liang, T.; Wang, Y.; Zeng, L.; Liu, Y.; Qiao, L.; Zhang, S.-f.; Zhao, R.; Li, G.; Zhang, R.; Xiang, J.; et al. Copper-doped 3D porous coating developed on Ti-6Al-4V alloys and its in vitro long-term antibacterial ability. *Appl. Surf. Sci.* **2020**, *509*, 144717.

19. Shivaram, A.; Bose, S.; Bandyopadhyay, A. Understanding long-term silver release from surface modified porous titanium implants. *Acta Biomater.* **2017**, *58*, 550–560. https://doi.org/10.1016/j.actbio.2017.05.048.
20. Pereira-Silva, P.; Borges, J.; Sampaio, P. Recent advances in metal-based antimicrobial coatings. *Adv. Colloid Interface Sci.* **2025**, *344*, 103590. https://doi.org/10.1016/j.cis.2025.103590.
21. Spriano, S.; Yamaguchi, S.; Baino, F.; Ferraris, S. A critical review of multifunctional titanium surfaces: New frontiers for improving osseointegration and host response, avoiding bacteria contamination. *Acta Biomater.* **2018**, *79*, 1–22. https://doi.org/10.1016/j.actbio.2018.08.013.
22. Liao, Y.; Wang, X.; Chen, P.; Zhong, Q.; Gong, J. Antimicrobial Mechanisms of Metal-Based Nanomaterials. *Int. J. Nanomed.* **2025**, *20*, 12879–12887. https://doi.org/10.2147/IJN.S557649.
23. Wang, C.; Wei, X.; Zhong, L.; Chan, C.L.; Li, H.; Sun, H. Metal-Based Approaches for the Fight against Antimicrobial Resistance: Mechanisms, Opportunities, and Challenges. *J. Am. Chem. Soc.* **2025**, *147*, 12361–12380. https://doi.org/10.1021/jacs.4c16035.
24. CLSI. Performance Standards for Antimicrobial Susceptibility Testing. In *CLSI Supplement M100*; CLSI: Wayne, PA, USA, 2026; Volume M100.
25. ASTM. Standard Test Method for Determining the Antimicrobial Activity of Immobilized Antimicrobial Agents Under Dynamic Contact Conditions. Available online: https://store.astm.org/e2149-13.html (accessed on 15 October 2026).
26. Akantibila, M.; Maurer, H.; Urban, M.; DiSpirito, S.; Torres, J.; Muhamed, A.; Harris, J.; Bharath, A.; Green, R.; Scabarozi, T.H.; et al. Silver (I) and Silver (II) Oxide Films for Biomedical Implants: Synthesis, Stability, Ion Release, and Antibacterial Efficacy. *J. Biomed. Mater. Res. A* **2025**, *113*, e38006. https://doi.org/10.1002/jbm.a.38006.
27. Edirisinghe, D.I.U.; D'Souza, A.; Ramezani, M.; Carroll, R.J.; Chicon, Q.; Muenzel, C.L.; Soule, J.; Monroe, M.B.B.; Patteson, A.E.; Makhlynets, O.V. Antibacterial and Cytocompatible pH-Responsive Peptide Hydrogel. *Molecules* **2023**, *28*, 4390. https://doi.org/10.3390/molecules28114390.
28. Fordham, W.R.; Redmond, S.; Westerland, A.; Cortes, E.G.; Walker, C.; Gallagher, C.; Medina, C.J.; Waecther, F.; Lunk, C.; Ostrum, R.F.; et al. Silver as a Bactericidal Coating for Biomedical Implants. *Surf. Coat. Technol.* **2014**, *253*, 52–57. https://doi.org/10.1016/j.surfcoat.2014.05.013.
29. Liang, J.; Wang, H.; Libera, M. Biomaterial surfaces self-defensive against bacteria by contact transfer of antimicrobials. *Biomaterials* **2019**, *204*, 25–35. https://doi.org/10.1016/j.biomaterials.2019.03.006.
30. von Eiff, C.; Jansen, B.; Kohnen, W.; Becker, K. Infections associated with medical devices: Pathogenesis, management and prophylaxis. *Drugs* **2005**, *65*, 179–214. https://doi.org/10.2165/00003495-200565020-00003.
31. Turner, R.J. The good, the bad, and the ugly of metals as antimicrobials. *Biometals* **2024**, *37*, 545–559. https://doi.org/10.1007/s10534-023-00565-y.
32. Lin, C.; Huang, X.; Xue, Y.; Jiang, S.; Chen, C.; Liu, Y.; Chen, K. Advances in medical devices using nanomaterials and nanotechnology: Innovation and regulatory science. *Bioact. Mater.* **2025**, *48*, 353–369. https://doi.org/10.1016/j.bioactmat.2025.02.017.
33. Jiang, H.; Li, L.; Li, Z.; Chu, X. Metal-based nanoparticles in antibacterial application in biomedical field: Current development and potential mechanisms. *Biomed. Microdevices* **2024**, *26*, 12. https://doi.org/10.1007/s10544-023-00686-8.
34. Mordorski, B.; Friedman, A. Chapter 4—Metal Nanoparticles for Microbial Infection. In *Functionalized Nanomaterials for the Management of Microbial Infection*; Boukherroub, R., Szunerits, S., Drider, D., Eds.; Elsevier: Boston, MA, USA, 2017; pp. 77–109.
35. Fernandez-Calvino, D.; Baath, E. Growth response of the bacterial community to pH in soils differing in pH. *FEMS Microbiol. Ecol.* **2010**, *73*, 149–156. https://doi.org/10.1111/j.1574-6941.2010.00873.x.
36. Gonzalez, J.M.; Aranda, B. Microbial Growth under Limiting Conditions-Future Perspectives. *Microorganisms* **2023**, *11*, 1641. https://doi.org/10.3390/microorganisms11071641.
37. Mougi, A. pH Adaptation stabilizes bacterial communities. *Npj Biodivers.* **2024**, *3*, 32. https://doi.org/10.1038/s44185-024-00063-5.
38. Ratkowsky, D.A.; Olley, J.; McMeekin, T.A.; Ball, A. Relationship between temperature and growth rate of bacterial cultures. *J. Bacteriol.* **1982**, *149*, 1–5. https://doi.org/10.1128/jb.149.1.1-5.1982.
39. Zwietering, M.H.; de Koos, J.T.; Hasenack, B.E.; de Witt, J.C.; van't Riet, K. Modeling of bacterial growth as a function of temperature. *Appl. Environ. Microbiol.* **1991**, *57*, 1094–1101. https://doi.org/10.1128/aem.57.4.1094-1101.1991.
40. Macia, M.D.; Rojo-Molinero, E.; Oliver, A. Antimicrobial susceptibility testing in biofilm-growing bacteria. *Clin. Microbiol. Infect.* **2014**, *20*, 981–990. https://doi.org/10.1111/1469-0691.12651.
41. Liu, H.; Wang, Y.; Zhang, Z.; Qi, H.; Zhang, Y.; Li, W.; Shi, Q.; Xie, X. Nutrient condition modulates the antibiotic tolerance of *Pseudomonas aeruginosa*. *Sci. Total Environ.* **2023**, *904*, 166749. https://doi.org/10.1016/j.scitotenv.2023.166749.

42. Park, H.J.; Kim, J.Y.; Kim, J.; Lee, J.H.; Hahn, J.S.; Gu, M.B.; Yoon, J. Silver-ion-mediated reactive oxygen species generation affecting bactericidal activity. *Water Res.* **2009**, *43*, 1027–1032. https://doi.org/10.1016/j.watres.2008.12.002.
43. Shimizu, K. Regulation Systems of Bacteria such as *Escherichia coli* in Response to Nutrient Limitation and Environmental Stresses. *Metabolites* **2014**, *4*, 1–35. https://doi.org/10.3390/metabo4010001.
44. Xu, X.; Ou, Z.M.; Wu, C.D. Growth Media Affect Assessment of Antimicrobial Activity of Plant-Derived Polyphenols. *Biomed. Res. Int.* **2018**, *2018*, 8308640. https://doi.org/10.1155/2018/8308640.
45. Bock, L.J.; Hind, C.K.; Sutton, J.M.; Wand, M.E. Growth media and assay plate material can impact on the effectiveness of cationic biocides and antibiotics against different bacterial species. *Lett. Appl. Microbiol.* **2018**, *66*, 368–377. https://doi.org/10.1111/lam.12863.
46. Taiyari, H.; Abu, J.; Zakaria, Z.; Omar, S.; Wen, C.Z.; Faiz, N.M. Different media affect the growth and antimicrobial minimum inhibitory concentrations of *Mycoplasma gallisepticum* and *Mycoplasma synoviae*. *J. Microbiol. Methods* **2026**, *240*, 107350. https://doi.org/10.1016/j.mimet.2025.107350.
47. Ramamoorthy, S.; Kushner, D.J. Binding of mercuric and other heavy metal ions by microbial growth media. *Microb. Ecol.* **1975**, *2*, 162–176. https://doi.org/10.1007/BF02010436.
48. Rewak-Soroczynska, J.; Dorotkiewicz-Jach, A.; Drulis-Kawa, Z.; Wiglusz, R.J. Culture Media Composition Influences the Antibacterial Effect of Silver, Cupric, and Zinc Ions against *Pseudomonas aeruginosa*. *Biomolecules* **2022**, *12*, 963. https://doi.org/10.3390/biom12070963.
49. De Leersnyder, I.; De Gelder, L.; Van Driessche, I.; Vermeir, P. Influence of growth media components on the antibacterial effect of silver ions on *Bacillus subtilis* in a liquid growth medium. *Sci. Rep.* **2018**, *8*, 9325. https://doi.org/10.1038/s41598-018-27540-9.
50. Gu, L.; Chen, Q.; Guo, A.; Liu, W.; Ruan, Y.; Zhang, X.; Nou, X. Differential Effects of Growth Medium Salinity on Biofilm Formation of Two *Salmonella enterica* Strains. *J. Food Prot.* **2020**, *83*, 196–203. https://doi.org/10.4315/0362-028X.JFP-19-418.
51. Seneviratne, C.J.; Yip, J.W.; Chang, J.W.; Zhang, C.F.; Samaranayake, L.P. Effect of culture media and nutrients on biofilm growth kinetics of laboratory and clinical strains of *Enterococcus faecalis*. *Arch. Oral. Biol.* **2013**, *58*, 1327–1334. https://doi.org/10.1016/j.archoralbio.2013.06.017.
52. Uhlich, G.A.; Chen, C.Y.; Cottrell, B.J.; Nguyen, L.H. Growth media and temperature effects on biofilm formation by serotype O157:H7 and non-O157 Shiga toxin-producing *Escherichia coli*. *FEMS Microbiol. Lett.* **2014**, *354*, 133–141. https://doi.org/10.1111/1574-6968.12439.
53. Wijesinghe, G.; Dilhari, A.; Gayani, B.; Kottegoda, N.; Samaranayake, L.; Weerasekera, M. Influence of Laboratory Culture Media on in vitro Growth, Adhesion, and Biofilm Formation of *Pseudomonas aeruginosa* and *Staphylococcus aureus*. *Med. Princ. Pract.* **2018**, *28*, 28–35. https://doi.org/10.1159/000494757.
54. Schifano, N.P.; Caputo, G.A. Investigation of the Role of Hydrophobic Amino Acids on the Structure-Activity Relationship in the Antimicrobial Venom Peptide Ponericin L1. *J. Membr. Biol.* **2022**, *255*, 537–551. https://doi.org/10.1007/s00232-021-00204-y.
55. Kohn, E.M.; Shirley, D.J.; Arotsky, L.; Picciano, A.M.; Ridgway, Z.; Urban, M.W.; Carone, B.R.; Caputo, G.A. Role of Cationic Side Chains in the Antimicrobial Activity of C18G. *Molecules* **2018**, *23*, 329. https://doi.org/10.3390/molecules23020329.
56. Wiegand, I.; Hilpert, K.; Hancock, R.E. Agar and broth dilution methods to determine the minimal inhibitory concentration (MIC) of antimicrobial substances. *Nat. Protoc.* **2008**, *3*, 163–175. https://doi.org/10.1038/nprot.2007.521.
57. Anderl, J.N.; Franklin, M.J.; Stewart, P.S. Role of antibiotic penetration limitation in *Klebsiella pneumoniae* biofilm resistance to ampicillin and ciprofloxacin. *Antimicrob. Agents Chemother.* **2000**, *44*, 1818–1824. https://doi.org/10.1128/AAC.44.7.1818-1824.2000.
58. Brown, D.C.; Turner, R.J. Assessing Microbial Monitoring Methods for Challenging Environmental Strains and Cultures. *Microbiol. Res.* **2022**, *13*, 235–257. https://doi.org/10.3390/microbiolres13020020.
59. Demidova, T.N.; Hamblin, M.R. Effect of cell-photosensitizer binding and cell density on microbial photoinactivation. *Antimicrob. Agents Chemother.* **2005**, *49*, 2329–2335. https://doi.org/10.1128/AAC.49.6.2329-2335.2005.
60. Goderecci, S.S.; Kaiser, E.; Yanakas, M.; Norris, Z.; Scaturro, J.; Oszust, R.; Medina, C.D.; Waechter, F.; Heon, M.; Krchnavek, R.R.; et al. Silver Oxide Coatings with High Silver-Ion Elution Rates and Characterization of Bactericidal Activity. *Molecules* **2017**, *22*, 1487. https://doi.org/10.3390/molecules22091487.
61. Wacogne, B.; Belinger Podevin, M.; Vaccari, N.; Koubevi, C.; Codjiova, C.; Gutierrez, E.; Davoine, L.; Robert-Nicoud, M.; Rouleau, A.; Frelet-Barrand, A. Concentration vs. Optical Density of ESKAPEE Bacteria: A Method to Determine the Optimum Measurement Wavelength. *Sensors* **2024**, *24*, 8160. https://doi.org/10.3390/s24248160.
62. Wang, H.H.; Isaacs, F.J.; Carr, P.A.; Sun, Z.Z.; Xu, G.; Forest, C.R.; Church, G.M. Programming cells by multiplex genome engineering and accelerated evolution. *Nature* **2009**, *460*, 894–898. https://doi.org/10.1038/nature08187.

63. Kaderabkova, N.; Mahmood, A.J.S.; Mavridou, D.A.I. Antibiotic susceptibility testing using minimum inhibitory concentration (MIC) assays. *NPJ Antimicrob. Resist.* **2024**, *2*, 37. https://doi.org/10.1038/s44259-024-00051-6.
64. Yang, D.D.; Paterna, N.J.; Senetra, A.S.; Casey, K.R.; Trieu, P.D.; Caputo, G.A.; Vaden, T.D.; Carone, B.R. Synergistic interactions of ionic liquids and antimicrobials improve drug efficacy. *iScience* **2021**, *24*, 101853. https://doi.org/10.1016/j.isci.2020.101853.

Disclaimer/Publisher's Note: The statements, opinions and data contained in all publications are solely those of the individual author(s) and contributor(s) and not of MDPI and/or the editor(s). MDPI and/or the editor(s) disclaim responsibility for any injury to people or property resulting from any ideas, methods, instructions or products referred to in the content.